

Self-structuring in Laser-Blow-Off Plasma Plume

Rajneesh Kumar

Abstract— This paper presents theoretical understanding of the experimentally observed oscillatory structures in the laser-blow-off (LBO) plasma plume. Oscillatory structures are formed without external sources (magnetic field, ambient gas, laser fluence, etc). A ablation mechanism of multi-component LiF-C (Lithium fluoride with carbon) thin film by laser-blow-off technique indicates that hydrodynamic instability (RT and KH) can grow during the melting process due to the different density and velocity of core plasma and surrounding materials (vaporized Li, F and C). It seems that instability grows with time and appears in the trailing portion of the plume. There is a sharp pressure gradient between front portion (first plasma) and trailing portion of plasma plume at the time of melt-through. Pressure gradient is the source of perturbation while negative differential conductance can be considered at the interface of plume front (high temperature) and trailing of plume (low temperature) during the free expansion of plume. This study invokes that hydrodynamic instability may be the source of self-structuring in LBO plasmas.

Index Terms—Laser ablation, laser-matter interaction, nonlinear waves, oscillations, instability in laser ablation, laser produced plasma, laser-blow-off plasma.

1 INTRODUCTION

Hydrodynamic instability has been interesting subject in the context of Inertial Confinement Fusion (ICF) since last few decades. However, such instabilities impose crucial limitations on symmetry and energy gain in fusion pellet implosions [1]. The ablative instability occurs near the front of an ablative heat wave, which accelerates the fusion shell. In this region opposed pressure and density gradient represent a standard Rayleigh-Taylor (R-T) unstable configuration, with important modifications arising from both mass and heat flow across the ablation front. The main difference between the ablative instability and its classical RT analog seems to be the presence of both, mass and heat flow across the unstable boundary [2-4]. Self-consistent description of RT instability has been established [5]. The process of ablative acceleration of plasma produced in thin foils and spherical pellets exposed to a high power laser radiation is hydrodynamically unstable because of growth of the Rayleigh-Taylor (RT) instability modes. The necessary condition for the RT instability- the oppositely directed pressure and density gradient is realized in the vicinity of the ablation front, where the absorbed energy of a laser beam is transported by the heat flux to the dense target layers. Recently thin-foil ablative-acceleration experiments [6-9] as well as the results of two-dimensional numerical simulations [10-12] have demonstrated substantial reduction of the instability growth rates compared to the classical theory predictions [13,14]. Another hydrodynamic instability due to velocity gradient (called K-H instability) is ubiquitous in high energy density physics such as Mach number shocks and jets, radioactive blast waves and radioactively molecular clouds, gamma-ray burts, accreting black holes [15] etc. The combined effect of RT-KH instability has been studied for destabilizing effects [16]. Therefore LPP plume evolution has been described by conventional hydro-

dynamics. It has been also noticed that at the time of evolution from initial to final stage the patterns [17] or fractals [18-19] are formed in LPP during free expansion of plume. However, self-patterning in discharge plasmas is manifestation for scientists [20, 21]. Fractal structure are self-organization process in plasma expansion [22, 23], as a result of a sequence of spontaneous symmetry-breaking process. Then a cascade self-organization scenario of the pattern genesis and evolution can be admitted [24]. Also, the dynamics of the transition of plasma from "disorder" to "order" needs a different type of description. Fractal structures have been investigated in the context of double layers [17] in convectional laser produced plasma (LPP).

Ablation mechanism of laser-blow-off (LBO) is slightly different from LPP, however self-structuring (oscillatory structures) in the trailing portion of LBO plume has been experimentally studied [25, 26]. Self-structuring depends on experimental conditions. This paper is aimed at presenting the theoretical understanding of the observed results. It is revealed that hydrodynamic instability (combined effect of RT and KH) grows in the trailing portion during the ablation (melting) while pressure gradient perturbed the instability so that a ion acoustic wave is formed. At the interface of two temperature plasmas [plume front (high temperature) and trailing portion (low temperature)] negative differential conductance (better explanation of negative floating potential and ion current) is also possible which induce the thermal fluctuations as well.

2. EXPERIMENTAL OBSERVATIONS

A detailed description of the experimental setup is reported in our earlier papers [27-29]. Only the main features of the setup are summarized here. The experiment was carried out in a stainless steel chamber, which was evacuated to a base pressure better than 2×10^{-5} mbar. Argon gas is introduced in the chamber at desired pressures through a fine-control needle valve. The target is composed of uniform layers of $0.05 \mu\text{m}$ of LiF film and $0.5 \mu\text{m}$ thick carbon film, deposited on a 1.2mm

• Rajneesh Kumar is currently working as a Project Scientist in Department of Physics, Indian Institute of Technology, Kanpur, UP, India PH-+91 8765696140. E-mail:rajneeshpr@gmail.com

thick quartz substrate. An Nd:YAG laser ($\lambda = 1.064 \mu\text{m}$) having a pulse width of 8 ns is used to ablate the thin film. The laser fluence ranging from 18 to 45 J/cm² is achieved by adjusting the operating parameters of the laser. The design, fabrication and assembly of the Triple Langmuir Probe (TLP) [30] used in the present study are described in the detailed in our previous report [26].

The plasma plume formed by the laser-blow-off of the LiF-C thin film using TLP and observed strong oscillation in the trailing portion of the floating potential and ion current profile have been observed [24]. For better understanding of experimental results, a typical profile of floating potential is shown in Fig.1.

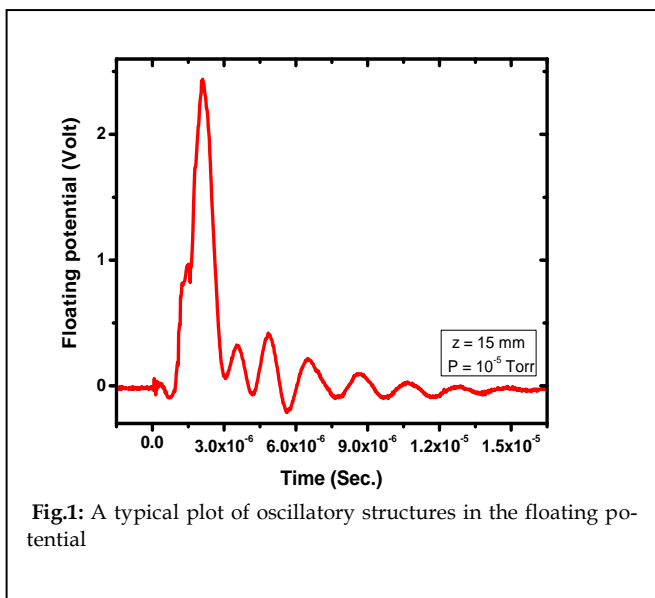


Fig.1: A typical plot of oscillatory structures in the floating potential

Systematic experiments are performed to understand the above phenomenon by studying the effect of different experimental parameters (ambient gas pressure, magnetic field, laser fluence etc.) on the growth of the observed oscillations. In order to study the axial propagation of the observed oscillations, the floating potential is observed at various distances (10 mm > z > 35 mm) away from the target surface. The amplitudes are normalized to its maximum value. Interestingly it is observed that oscillation amplitude increases up to a distance of z = 25 mm and then starts decreasing with further increase in the probe position as shown in Fig.2. This observation indicates the growth of instability.

3. THEORETICAL MODEL

An adequate description of laser energy deposition which occurs on a time scale of tens of nanoseconds and on a spatial scale on the order of micrometers while plasma plume at the final stage of expansion that takes place microseconds and centimeters away from the initial event. Hence plasma plume

evolution includes two important parts- the initial stage is one or two dimensional where laser spot large compared to skin depth and the final one consists of three dimensional expansion [31-33]. The initial one-dimensional stage occurs during laser deposition followed by the very first moments of the expansion. The longitudinal size of the hot material is still much

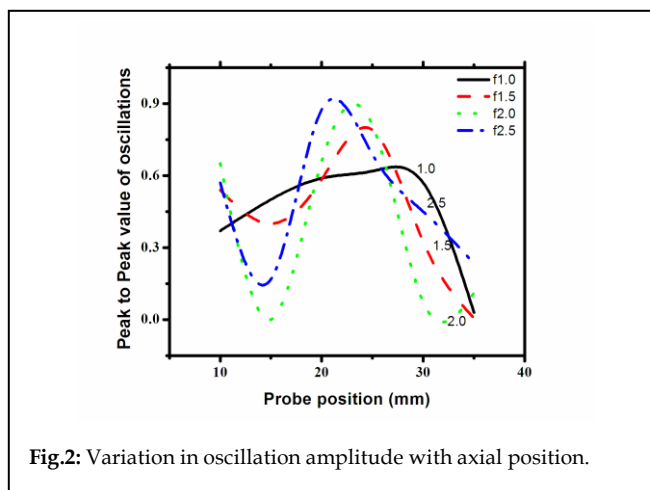


Fig.2: Variation in oscillation amplitude with axial position.

smaller than the transverse size determined by the laser spot. Clearly, laser-material interaction, ionization, energy and material transport are the significant effects during this period. After some time, the plasma cloud becomes truly three dimensional, but the physics simplifies considerably. At this stage, plume evolution can be described by conventional hydrodynamics and is sensitive only to integral parameters of the laser pulse. Hence fractal structures and self-structuring have been studying in laser produced plasmas due to its manifestation of the universality of process in plasma free expansion in short scale of time and space. Such studies suggests that laser produced plasmas are self-consistently stratified in the time of ablation and expansion. Stratification can be explained / caused by the hydrodynamic instability. Let us briefly discuss about hydrodynamic instabilities (types of R-T and K-H instabilities) during laser ablation mechanism and self-structuring in the plume expansion of laser-blow-off plasma plume of thin film. It is well accepted that the process of ablative acceleration of a plasma produced in thin films and spherical pellets exposed to a high-power laser radiation is hydrodynamic unstable because of growth of the R-T instability. Here we restrict our attention to a narrow region around the ablation front derive steady ablation profiles from the incompressible fluid model. Although good amount of work has been done on plume dynamics of LBO plasma, however laser- target (LiF-C) interaction is not fully understood. Hence we will start our discussion from melting process to free expansion of LBO plume. Let us consider a plasma with ions of mass m_i and charge Z . The pressure p , density ρ , temperature T , specific enthalpy ξ and specific heat at constant pressure c_p are as-

sumed for an idial gas with adiabatic index γ hence

$$p = \frac{\rho T}{M} \quad \xi = c_p T, \quad c_p = \frac{1}{M} \frac{\gamma}{\gamma-1}, \quad M = \frac{m_i}{1+z} \quad (1)$$

The basic assumptions of the fluid model can be expressed by the equation of energy conservation. The approximation of small pressure variation leads us to consider the divergence-free energy equation [5]

$$\nabla \cdot (\rho \xi V + q) = 0 \quad (2)$$

Here V denotes the fluid velocity and $q = -K \nabla T$ the heat flow. Generally, the coefficient of heat conductivity K is a function of ρ and T and can be assumed as an arbitrary power law $K = cont T^\delta (\rho T)^{-e}$. Supposing constant pressuer, the density dependence can be eliminated by the equation of state (Eq.1) and it is therefore sufficient to consider a temperature dependent heat conductivity, $K = CT^\delta$, only. Specifically, for electronic heat conduction one has $\delta=5/2$ and $e = 0$. The energy equation (2) is an obvious generalization of the usual incompressibility condition $\nabla \cdot V = 0$. It can be shown briefly that Eq. (2) follows from the general energy equation when pressure variation is neglected. The rate of the change of the specific entropy s as a result of heat flow can be given as

$$\rho T \frac{ds}{dt} + \nabla \cdot q = 0, \text{ and } \frac{d}{dt} = \partial_t + V \cdot \nabla \quad (3)$$

Using the first law of thermodynamics $d\xi = T ds + dp/\rho$, Eq. (1) yields

$$\rho T ds = -c_p T d\rho + (c_p M - 1) dp \quad (4)$$

We further express the density change by the equation of continuity

$$\frac{d\rho}{dt} + \rho \nabla \cdot V = 0 \quad (5)$$

By inserting Eqs (4) and (5) into Eq. 3 one can find

$$\nabla \cdot (\rho \xi V + q) + (c_p M - 1) \partial_t p - V \cdot \nabla p = 0 \quad (6)$$

This equation is similar to Eq.(2) at constant pressure (last two terms will be vanished). We now consider the incompressible fluids in a gravitational field ignoring the viscosity, surface tension, and heat transfer and introduce a Cartesian coordinate system. The fluids have continuous density $\rho(y)$, pressure $p(y)$ and velocity $u(y)$ profiles initially and the pressure $p(y)$ satisfies the static equilibrium condition

$$\frac{dp(y)}{dy} = -\rho(y)g \quad (7)$$

Where, g is the gravitational acceleration. The fluid dynamics is governed by

$$\frac{\partial \rho}{\partial t} + u \frac{\partial \rho}{\partial x} + v \frac{\partial \rho}{\partial y} = 0 \quad (8)$$

$$\rho \left(\frac{\partial u}{\partial t} + u \frac{\partial u}{\partial x} + v \frac{\partial u}{\partial y} \right) = -\frac{\partial p}{\partial x} \quad (9)$$

$$\rho \left(\frac{\partial v}{\partial t} + u \frac{\partial v}{\partial x} + v \frac{\partial v}{\partial y} \right) = -\frac{\partial p}{\partial y} - \rho g \quad (10)$$

$$\frac{\partial u}{\partial x} + \frac{\partial v}{\partial y} = 0 \quad (11)$$

Where u and v is the velocity in x-direction and y-direction respectively. Equations are linearised and perturbed quantity v^1 is yield [16]

$$(n + iku^0)^2 \left(\rho^0 \frac{d^2 \tilde{v}}{dy^2} + \frac{d\rho^0}{dy} \frac{d\tilde{v}}{dy} - k^2 \rho^0 \tilde{v} \right) - ik(n + iku^0) \left(\frac{d\rho^0}{dy} \frac{du^0}{dy} + \rho^0 \frac{d^2 u^0}{dy^2} \right) \tilde{v} + k^2 g \frac{d\rho^0}{dy} \tilde{v} = 0 \quad (12)$$

Where $k = 2\pi/\lambda$ is the wave number and $n = \gamma - i\omega$ where γ and ω are linear growth rate and frequency. Eq. (12) combined with appropriate boundary conditions forms an Eigen value problem. It is the standard form of interface instability for continuous interface profiles [34, 35]. Let $g = 0$ and $d\rho^0/dy = 0$, the inviscid RT equation [17] is obtained

$$(n + iku^0) \left(\frac{d^2 \tilde{v}}{dy^2} - k^2 \tilde{v} \right) - ik \frac{d^2 u^0}{dy^2} \tilde{v} = 0 \quad (13)$$

Approximate Eigen function are

$$\tilde{v}(y) = [n + iku^0(y)] e^{-k|y|} \quad (14)$$

Let $u^0 = 0$, the characteristic equation used in the RT instability with continuous density profiles can be yielded.

$$n^2 \left(\rho^0 \frac{d^2 \tilde{v}}{dy^2} + \frac{d\rho^0}{dy} \frac{d\tilde{v}}{dy} - k^2 \rho^0 \tilde{v} \right) + k^2 g \frac{d\rho^0}{dy} \tilde{v} = 0 \quad (15)$$

However our case can be solved by using the Eq. (12). Let us write the constant plus exponential density and velocity profiles [36, 37] when plume passes from the carbon layer (see Fig.3)

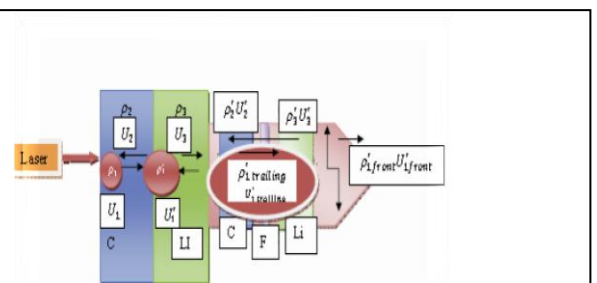


Fig.3: Diagram showing the velocity and density of different components during melting of LIF-C target and free expansion in the vacuum.

$$\rho(0) = \rho_1 - \frac{\rho_1 - \rho_2}{2} e^{-y/L_\rho}, \quad \text{when } y > 0 \quad (16)$$

$$\rho(0) = \rho_2 + \frac{\rho_1 - \rho_2}{2} e^{y/L_\rho} \quad \text{where } y < 0 \quad (17)$$

Similarly for velocities

$$u(0) = U_1 - \frac{U_1 - U_2}{2} e^{-y/L_u} \quad \text{where } y > 0 \quad (18)$$

$$u(0) = U_2 + \frac{U_1 - U_2}{2} e^{y/L_u} \quad \text{where } y < 0 \quad (19)$$

Where L_ρ and L_u are density and velocity gradient scale lengths, respectively. The density (velocity) is discontinuous at $y=0$ when $L_\rho = 0$ ($L_u = 0$). The density (velocity) is homogenous when $L_\rho = +infinite$ and $L_u = infinite$. ρ_1 and ρ_2 is the density away from the interface of the upper (lower) fluid. U_1 and U_2 are velocities away from the interface in x-direction of the upper and lower fluids, respectively.

The growth rate of classical RT-KH synthesis instability assuming $L_\rho = L_u = 0$, can be obtained as [16]

$$\gamma = -ik \frac{\rho_1 U_1 + \rho_2 U_2}{\rho_1 + \rho_2} + \sqrt{\frac{\rho_1 \rho_2 k^2 (U_1 - U_2)^2 + k g (\rho_1^2 - \rho_2^2)}{(\rho_1 + \rho_2)^2}} \quad (20)$$

There is a transverse interface of two medium of carbon and lithium fluoride, hence when plume enters in the medium of LiF from C. Plume character in this situation will be different (See Fig.3)

The growth of the R-T instability when plume enters in LiF layer (a different medium from earlier)

$$\eta_1^2 = k_1 a \frac{\rho_1' - \rho_3}{\rho_1 + \rho_3} \quad (21)$$

And growth rate of K-H instability is (due to different velocity due to different atomic weight)

$$\gamma_1 = k_1 |U_1' - U_3| \sqrt{\frac{\rho_1 \rho_3}{(\rho_1 + \rho_3)}} \quad (22)$$

Let us find out the dispersion relation for R-T and K-H instability. Hence write down the expression for modified density and velocity

$$\rho'(0) = \rho_1' - \frac{\rho_1' - \rho_3}{2} e^{-y'/L_\rho'} \quad \text{where } y' > 0 \quad (23)$$

$$\rho'(0) = \rho_3 + \frac{\rho_1' - \rho_3}{2} e^{-y'/L_\rho'} \quad \text{where } y' < 0 \quad (24)$$

$$u'(0) = U_1' - \frac{U_1' - U_3}{2} e^{-y'/L_u'} \quad \text{where } y' > 0 \quad (25)$$

$$u'(0) = U_3 + \frac{U_1' - U_3}{2} e^{y'/L_u'} \quad \text{where } y' < 0 \quad (26)$$

Where L_ρ' and L_u' are density and velocity gradient scale lengths in LiF layer, respectively. The density (velocity) is discontinuous at $y = 0$ when $L_\rho' = 0$ and $L_u' = 0$. The density (velocity) is homogenous when $L_\rho' = +infinite$ and $L_u' = infinite$. ρ_1' and ρ_3 is the density away from the interface of the upper (lower) fluid. U_1' and U_3 are velocities away from the interface in y-direction of the upper and lower fluids, respectively.

The growth rate of classical RT-KH synthesis instability assuming $L_\rho' = 0 = L_u' = 0$, can be obtained as

$$\gamma_1 = -ik_1 \frac{\rho_1' U_1' + \rho_3 U_3}{\rho_1' + \rho_3} + \sqrt{\frac{\rho_1' \rho_3 k_1^2 (U_1' - U_3)^2 + k_1 g (\rho_1'^2 - \rho_3^2)}{(\rho_1' + \rho_3)^2}} \quad (27)$$

Hence RT-KH instability grows in the vaporized materials (trailing portion of plume) during the melting process of LiF-C film. This instability can be stratified the plasma when it freely expands in vacuum so that layers of different material with different density and different velocity propagate. Due to instability or sequential film removal there are fast and slow velocity component in the plume. When fast component ignites to the vacuum it highly perturbed the slow portion. There is a sharp pressure gradient between fast and slow component. There are two types of perturbation will be felt by trailing portion of the plume at the time of leaving the LiF surface (melt-through): (1) Sharp pressure difference at the surface or adiabatic free expansion (See Fig. 4)

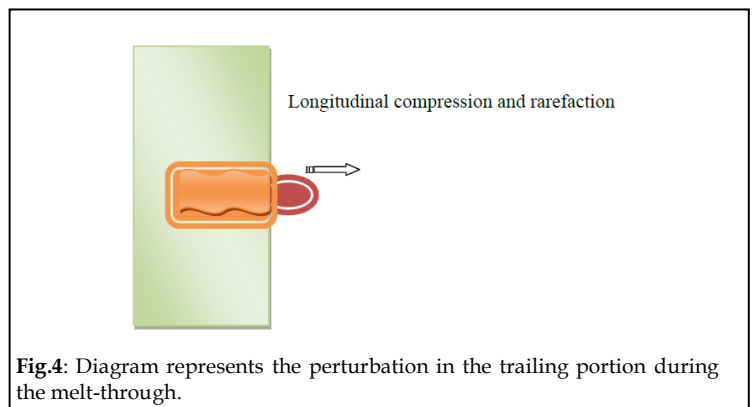


Fig.4: Diagram represents the perturbation in the trailing portion during the melt-through.

(2) There is a pressure difference between front and trailing portion.

However front portion is not affected and trailing portion which is made by neutrals is highly stratified. This stratification enhances the RT-KH instability in the trailing portion. There is a sharp pressure gradient between front and trailing portion which perturb the RT-KH instability in trailing portion. Hence we measure the perturbation in floating poten-

tial as an oscillatory profile. R-T and K-H instability will be continue in the free expansion where plasma plume will move against to the surrounding of stratified medium of different velocity and gradients. Hence growth rate in each segment or layer can be written. RT and KH instability growth rate due to plasma plume and Li atom (material) medium (See Fig.5)

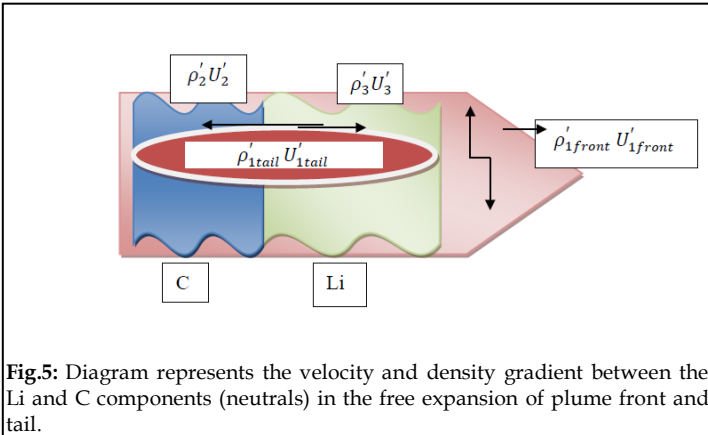


Fig.5: Diagram represents the velocity and density gradient between the Li and C components (neutrals) in the free expansion of plume front and tail.

$$\gamma_{1L} = -ik_{1Li} \frac{\rho'_{1tail} U'_{1tail} + \rho'_3 U'_3}{\rho_{1tail} + \rho_3} + \sqrt{\frac{\rho'_{1tail} \rho'_3 k_{1Li}^2 (U'_{1tail} - U'_3)^2 + k_{1Li} g (\rho'_{1tail} - \rho'_3)^2}{(\rho_{1tail} + \rho_3)^2}} \quad (28)$$

And instability due between plasma plume and surrounding of Carbon atoms

$$\gamma_{1c} = -ik_{1c} \frac{\rho'_{1tail} U'_{1tail} + \rho'_2 U'_2}{\rho_{1tail} + \rho_2} + \sqrt{\frac{\rho'_{1tail} \rho'_2 k_{1c}^2 (U'_{1tail} - U'_2)^2 + k_{1c} g (\rho'_{1tail} - \rho'_2)^2}{(\rho_{1tail} + \rho_2)^2}} \quad (29)$$

Hence total growth rate of instability is

$$\gamma' = \gamma_{1L} + \gamma_{1c} \quad (30)$$

This approximation can be simplified by assuming RT instability due to carbon layer because carbon layer (0.5 micrometer) is 10 times higher than LiF (0.05 micrometer) layer in the target. In the free expansion we can ignore the stratification of plume. In free expansion we also can assume only core fluid (ions/electrons) and outer fluid (neutrals), means there is no individual effect of C and Li, if we ignore the atomic weight effect during plume expansion.

Hence instability growth rate in the target

$$\gamma = \gamma_1 \quad (31)$$

And total instability in free expansion

$$\gamma' = \gamma_{1L} \quad (32)$$

Or

$$\gamma' = \gamma_{1c} \quad (33)$$

Here it is important to know that number of carbon neutrals should be 10 times higher than the Li neutrals. It is highly possible that Li atoms are in front portion or faster than carbon. Hence in the discussion of trailing portion we must consider the carbon neutrals.

$$\text{Hence } \gamma' = \gamma_{1c} \quad (34)$$

So far we have demonstrated that R-T and K-H instability is perturbed and oscillates the floating potential in real and practical system. It seems that at a particular position, radial density gradient between core and surrounding is higher than their velocities hence R-T instability may play much role than K-H instability.

The growth of the R-T instability is written as

$$\lambda^2 = ka \frac{\rho_i - \rho_c}{\rho_i + \rho_c} \quad (35)$$

or

$$\lambda = \pm ka \left(\frac{\rho_i - \rho_c}{\rho_i + \rho_c} \right)^{1/2} \quad (36)$$

Where k is the perturbation wave number, a is the acceleration and ρ_i and ρ_c are the density of the ions and ablated carbon material (neutrals) respectively.

Up to now we have considered that plasma plume ($\rho_e = \rho_i$) and ablated material (neutrals of carbon and Lithium) are two incompressible mediums of two relative density and velocity, hence RT-KH instability is produced at the interface of these two medium. In the real / practical system there are several collisions among plasma species and ablated materials. Sometimes, neutrals and plasma are formed due to their collisions, which affect the plume expansion. Instability is produced at the interface and perturbation propagate in the upper medium (outer medium of neutrals), which has lower density than lower medium (core medium of ions). Hence our interest is to see the collisional effect in the upper medium and how instability growth rate is modified after encountering the collisions. There is a fewer chance of presence of neutrals in the core, hence we ignore this effect. Let us write the diffusion equations for ions and neutrals with their source terms.

The one-dimensional diffusion equations (along axial direction) for the electrons and neutral atoms can be written as

$$\frac{\partial \rho_i}{\partial t} - D \frac{\partial^2 \rho_i}{\partial y^2} = Q_i, \rho_n \quad (37)$$

and

$$\frac{\partial \rho_n}{\partial t} - D\theta \frac{\partial^2 \rho_n}{\partial y^2} = S(\rho_i, \rho_n) \quad (38)$$

Where, ρ_i is the ion density (assuming equal to the electron density), ρ_n is the density of neutral atoms, Q and S are the rates of creation of ions and atoms respectively, D is the diffusion coefficient for the electrons & ions, and θ is the ratio of the diffusion coefficient of the atoms to that of the ions. By considering the possible atomic processes, which are responsible for creation or diffusion of ions and neutrals; the quantity Q and S can be expressed as-

$$Q(\rho_i, \rho_n) = \rho_n Q_2(\rho_i) + \eta S^2 + \zeta \rho_i^2 + Q_3(\rho_i) - \gamma \rho_i - \xi \rho_i \quad (39)$$

and

$$S(\rho_i, \rho_n) = Q_1(\rho_i) - \Lambda \rho_n Q_2(\rho_i) - \delta \rho_n - 2\eta \rho_n^2 \quad (40)$$

The term $\rho_n Q_2(\rho_i)$ in Eq. (39) represents the loss of atoms due to electron impact ionization and therefore it is reflected in the term $\rho_n Q_2(\rho_i)$ in the Eq. (39) as enhancement number density of ions. $Q_2(\rho_i)$ depends on ρ_i because the collision frequency is proportional to ρ_i and factor Λ is greater than one because not all the atoms become ions. $Q_1(\rho_i)$ is the rate of creation of atoms per unit volume by laser ablation from the target. The terms $\gamma \rho_i$ and $\delta \rho_n$, respectively, represent the loss of ions and atoms due to radial diffusion, where γ and δ are depend on the radial diffusion coefficient and plume geometry. The terms in $\eta \rho_n^2$ and $\zeta \rho_i^2$ represent the loss of atoms as well as ions due to the atom-atom collisions and electron-ion recombination respectively. The term $Q_3(\rho_i)$ represents the direct ionization of atoms by laser intensity.

$$Q(\rho_{i0}, \rho_{n0}) = 0 \quad (41)$$

and

$$S(\rho_{i0}, \rho_{n0}) = 0 \quad (42)$$

We have consider the plume dimension to define the boundary condition along the y - direction, which can be taken as $y = 0, L$, where L is the length of plume. Therefore in the present case, boundary conditions can be assumed as

$$\rho_i(y=0, t) = \rho_i(y=L, t) = \rho_{i0} \quad (43)$$

and

$$\rho_n(y=0, t) = \rho_n(y=L, t) = \rho_{n0} \quad (44)$$

Since, the present interest is to see the perturbations in density away from ρ_{i0} and ρ_{n0} , so that the ρ_i and ρ_n can be written as

$$\rho_i = \rho_{i0} + \tilde{\rho}_i(y, t) \quad (45)$$

and

$$\rho_n = \rho_{n0} + \tilde{\rho}_n(y, t) \quad (46)$$

Where, $\tilde{\rho}_i$ and $\tilde{\rho}_n$ are the perturbations in ions and neutrals densities respectively. Let us assume that the boundary conditions is homogeneous Dirichlet boundary conditions for the perturbations $\tilde{\rho}_i$ and $\tilde{\rho}_n$, so that

$$\tilde{\rho}_i(y=0, t) = \tilde{\rho}_i(y=L, t) = 0 \quad (47)$$

$$\tilde{\rho}_n(y=0, t) = \tilde{\rho}_n(y=L, t) = 0 \quad (48)$$

The liner stability analysis is carried out by substituting above equations in Eqs.(37) and (38), and then linearized to obtain

$$\frac{\partial \tilde{\rho}_i}{\partial t} = \frac{\partial Q}{\partial \rho_i} \tilde{\rho}_i + \frac{\partial Q}{\partial \rho_n} \tilde{\rho}_n + D \frac{\partial^2 \tilde{\rho}_i}{\partial y^2} \quad (49)$$

and

$$\frac{\partial \tilde{\rho}_n}{\partial t} = \frac{\partial S}{\partial \rho_i} \tilde{\rho}_i + \frac{\partial S}{\partial \rho_n} \tilde{\rho}_n + \theta D \frac{\partial^2 \tilde{\rho}_n}{\partial y^2} \quad (50)$$

Here all derivatives of Q and S are evaluated at the steady state ρ_{i0} and ρ_{n0} , and subscript 0 is dropped. Eqs (49) and (50) can be solved in terms of modes as,

$$\tilde{\rho}_i(y, t) = \tilde{\rho}_{in} e^{\lambda_n t} \sin \frac{n\pi y}{L} \quad (51)$$

$$\tilde{\rho}_n(y, t) = \tilde{\rho}_{nn} e^{\lambda_n t} \sin \frac{n\pi y}{L} \quad (52)$$

The profiles of perturbed densities are shown in Fig. 6, which are quite similar to our experimental observations that oscillations are nearly in sinusoidal profile after 3 μ s.

For further study by combining Eq. 51, 52 and 49, 50, we get,

$$\begin{bmatrix} -\lambda_n + Q_{\rho_i} - D \frac{n^2 \pi^2}{L^2} & Q_{\rho_n} \\ S_{\rho_i} & -\lambda_n + S_{\rho_n} - \theta D \frac{n^2 \pi^2}{L^2} \end{bmatrix} \begin{bmatrix} \tilde{\rho}_{in} \\ \tilde{\rho}_{nn} \end{bmatrix} = 0 \quad (53)$$

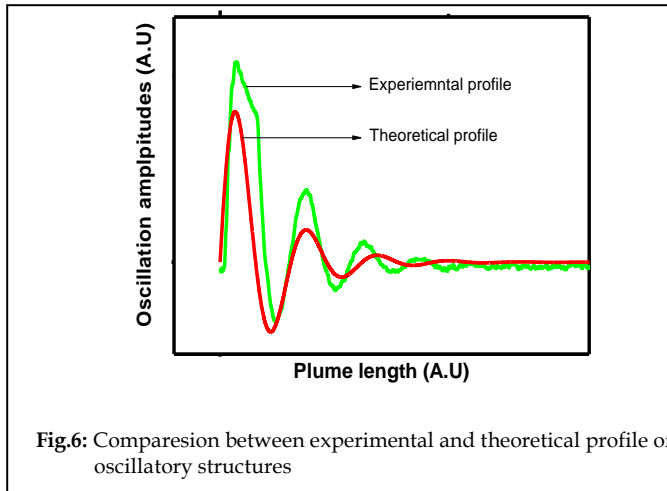


Fig.6: Comparison between experimental and theoretical profile of oscillatory structures

In the present case, it is difficult to approximate the uniform real steady state, therefore, the equivalent Eqs. of 51,52 and 53 would have been much more complicated. To find a nontrivial solution for Eq. (53), the determinant of the matrix need to be zero, Hence

$$\lambda_n^2 - \lambda_n \left[Q_{\rho_i} + S_{\rho_n} - (1+\theta)D \frac{n^2 \pi^2}{L^2} \right] + \left(Q_{\rho_i} - D \frac{n^2 \pi^2}{L^2} \right) \left(S_{\rho_n} - \theta D \frac{n^2 \pi^2}{L^2} \right) - Q_{\rho_n} S_{\rho_i} = 0 \quad (54)$$

or, the Eq. (54) can be expressed in terms of the trace H_n and the determinant I_n of the matrix in with $\lambda_n = 0$,

$$\lambda_n^2 - \lambda_n H_n + I_n = 0 \quad (55)$$

Eq. (55) determines the roots of λ_n ,

$$\lambda_n^\pm = \frac{1}{2} \left[H_n \pm \sqrt{H_n^2 - 4I_n} \right] \quad (56)$$

$$\lambda_n^\pm = \frac{1}{2} H_n \pm \frac{1}{2} \sqrt{H_n^2 - 4I_n} \quad (57)$$

where

$$H_n = S_{\rho_n} + Q_{\rho_i} - \left(\frac{D\pi^2}{L^2} \right) n^2 (1+\theta) \quad (58)$$

and

$$I_n = \frac{\theta n^4 D \pi^2}{L^4(z)} - (\theta Q_{\rho_i} + S_{\rho_n}) \frac{n^2 D \pi^2}{L^2} + Q_{\rho_i} S_{\rho_n} - Q_{\rho_n} S_{\rho_i} \quad (59)$$

Above equations (Eq.58 and 59) can be written as

$$I_n = \frac{\theta n^4}{\mu^2} - \left(Q_{\rho_i} + S_{\rho_n} \right) \frac{n^2}{\mu} + Q_{\rho_i} S_{\rho_n} - Q_{\rho_n} S_{\rho_i} \quad (60)$$

$$H_n = S_{\rho_n} + Q_{\rho_i} - \left(\frac{1}{\mu} \right) n^2 (1+\theta) \quad (61)$$

where

$$\mu = \frac{L^2}{D\pi^2} \quad (62)$$

where μ can be defined as a bifurcation parameter, which depends on the length of the plume, L and diffusion coefficient, D .

Stable and unstable modes can be easily understood from Eq. (61). The mode characterized by n is stable if $\text{Re } \lambda_n < 0$ and unstable if $\text{Re } \lambda_n > 0$. The stability of the system can also be expressed in terms of bifurcation parameter (μ) as-

$$\mu < \frac{n^2 (1+\theta)}{S_{\rho_n} + Q_{\rho_i}} \text{ stable mode} \quad (63)$$

$$\mu > \frac{n^2 (1+\theta)}{S_{\rho_n} + Q_{\rho_i}} \text{ unstable mode} \quad (64)$$

In the above discussion we have seen that trailing portion of plume is perturbed and RT instability (we consider only density gradient between plasma plume and surroundings) appears in the sense of oscillations. Stable modes are found in front portion while unstable modes appear in the trailing portion. Several issues are not addressed in the above discussion. (1) What is the role of velocity (temperature) difference between plasma plume and surrounding? Surrounding will be considered as trailing portion. (2) Negative value of floating potential and ion current in the profiles?

Velocity of ions can also be perturbed by applied electric field on the tip of probe. Let us discuss it using scale relativity theory [38]. We have two plasmas of different velocities or temperatures (plume front and tail), the interface dynamics is described by the coupled equation set

$$iD \frac{\partial \psi_1}{\partial t} = \beta T_1 \psi_1 + \Gamma \psi_2 \quad (65)$$

$$iD \frac{\partial \psi_2}{\partial t} = \beta T_2 \psi_2 + \Gamma \psi_1 \quad (66)$$

Where ψ_1, ψ_2 are the wave functions of the plasmas (front and trailing), T_1 and T_2 is specific temperatures of the plasmas and β and Γ are two constants [24,39].

Using the wave functions $\psi_1 = \sqrt{\rho_1} e^{i\phi_1}$ and $\psi_2 = \sqrt{\rho_2} e^{i\phi_2}$. Putting the values in above Eqs. 65, 66 and separate the real and imaginary parts with considering $\rho_1 = \rho_2$, phase difference $\delta = \phi_1 - \phi_2$ while temperature $T = T_1 - T_2$, ion current can be obtain as [22]

$$I = I_M \sin \left(\delta_0 - \frac{\beta}{D} \int T dt \right) \quad (67)$$

Where δ_0 an integration constant and I_M the current amplitude. Eq. 67 is similar to Eq. 51. Above equation reproduces a dc Josephson thermal type effect if $T = 0$ or ac Josephson thermal type effect if $T \neq 0$, i. e., oscillations of current with the pulsation

$$\omega = \frac{\beta T}{D} \quad (68)$$

Since any time-dependent local thermal energy fluctuation (e.g for the plasma expansion these fluctuations are induced by the cooling process [16]) admits a Fourier discrete decomposition [40] of the form

$$T = T_0 + \bar{T}_0 \cos(\Omega t), \quad \bar{T}_0 \ll T \quad (69)$$

Using the triple probe theory that floating potential can be estimated as

$$V_f = \frac{T}{\ln 2} \quad (70)$$

Hence

$$V_f = V_0 + \bar{V}_0 \cos(\Omega t) \quad (71)$$

$$V_{f_{trailing}} = \bar{V}_0 \cos(\Omega t) \quad (72)$$

Eq. (72) indicates that trailing portion floating potential profile oscillates with certain frequency which has been also observed in Ref. [25].

Then, by substituting Eq. (69) to Eq. (67) and integrating it, the expression for the current becomes

$$I = I_M \sum_{n=-\infty}^{+\infty} (-1)^n J_n \left(\frac{\beta \bar{T}_0}{D \Omega} \right) \sin \left[\left(n \Omega - \frac{\beta T_0}{D} \right) t + \delta_0' \right] \quad (73)$$

Where J_n is the n^{th} -order Bessel function [40] and δ_0' a new integration constant.

When the pulsation $\Omega_0 = \beta T_0 / D$, satisfy the relation

$$\Omega_0 = n \Omega \quad (74)$$

The temporal average of $I = \langle I(t) \rangle$ differs from zero, i. e there is a continuous component of the current of the form

$$I_c = (-1)^n I_M J_n \left(\frac{\beta \bar{T}_0}{D \Omega} \right) \sin(\delta_0') \quad (75)$$

Eq. (75) can interprets oscillatory ion current, which has been measured and reported in Ref. [26]. Negative profile of ion

current can also be described. From above Eq. (75) peaks of the continuous current for temperatures

$$T_n = n \bar{T}, \bar{T} = D \Omega / \beta, T_n = D \Omega_0 / \beta, n = 1, 2, 3, \dots \quad (76)$$

and consequently a negative differential conductance $\frac{dI}{\beta T_0} < 0$. Moreover from above equation, the intensity current of the peak n varies continuously in the range of $\pm I_M J_n(\beta \bar{T}_0 / D \Omega)$ at constant temperature $n \bar{T}$, and the phase varies in range $-\frac{\pi}{2}$ to $+\frac{\pi}{2}$. This means that, in the interface, thermal energy is generated or absorbed. Consequently, the self-structuring of the interface as a double layer appears by means of a negative differential conductance [41-43] and temperature fluctuations [44] induce the oscillations. Hence we get negative profile of floating potential and ion current.

4 CONCLUSIONS

Hydrodynamic instability (RT-KH) grows in the trailing portion of ablated material during melting of LiF-C film. Trailing portion is highly perturbed at the time of melt-through and strong oscillations are formed in trailing portion which remains during free expansion in vacuum. Theoretically obtained perturbed ion current is quite matched with experimentally observed profile. At the interface of plume front (high temperature plasma) and trailing portion (low temperature plasma), thermal energy is generated or absorbed. Hence, negative profile of floating potential (electron temperature) and ion current form. Our study reveals that hydrodynamic instability is the source of self-structuring in the Laser-blow-off plasmas of multi-component target.

ACKNOWLEDGMENT

The authors wish to thank Dr. Ajay Kumar and Dr. R. K. Singh, Institute for Plasma Research, Gandhinagar, India for help in experiment and discussion.

REFERENCES

- [1] J. D. Lindl and W. C. Mead, 'Two dimensional simulation of fluid instability in laser-fusion pallet', *Phys. Rev. Lett.*, vol. 34, issue 20, pp-1273-1276, 1975.
- [2] S. A. Orszag, Vortex Simulations of the Rayleigh-Taylor", *Phys. Fluids*, vol. 25, pp 1653-1668, 1982.
- [3] M. H. Emery, J. H. Gardner and J. P. Boris, Rayleigh-Taylor and Kelvin-Helmoltz in targets accelerated by laser ablation', *Phys. Rev. Lett.*, vol. 48, issue 10, pp 677-680, 1982.
- [4] R. G. Evans, A. J. Bennet and G. J. Pert, " Rayleigh-Taylor instability in laser-accelertaed targets', *Phys. Rev. Lett.*, vol.49, issue 22, pp1639-1642, 1982.
- [5] H. J. Kull and S. I. Anisimov., Ablative stabilization in the incompressible Rayleigh-Taylor instability, *Phys. Fluids*, vol. 29 issue 7, pp 2067-2075, 1986.
- [6] J. D. Kilkenny., Experiemntal results on hydrodynamic instabilities in

- laser accelerated planar packages', *Phys. Fluids B*, vol. 2, issue 6, pp 1400-1404, 1990.
- [7] J. Grun, et al, Rayleigh-Talor instability growth rates in targets accelerated with a laser beam, *Phys. Rev. Lett.*, vol. 58, issue 25, pp 2672-2675, 1987.
- [8] H. Nishimura, H. Takabe, K. Mima, Hydrodynamic instability in an ablatively imposed target irradiated by high power green lasers, *Phys. Fluids*, vol.31, issue 10, pp 2875-2884, 1988.
- [9] R. L. McCarty, et al, Laser compression and instability in inertial confinement fusion, *Plasma Phys. Contr. Fusion*, vol. 31, issue 10, pp 1517-1533, 1989.
- [10] M. H. Emery, J. H. Gardner and S. E. Bodner, Rapaport replies, *Phys. Rev. Lett.*, vol. 62, issue 6, pp 692-695, 1989.
- [11] M. Tabak, D. H. Munro and J. P. Lindl, Hydrodynamic stability and direct drive approach to laser fusion, *Phys. Fluids B*, vol. 2, issue 5 pp 1007-1015, 1990.
- [12] M. H. Emery, J. P. Dahlburg and J. H. Gardner, The Rayleigh-Taylor instability in ablatively accelerated targets with 1, 1/2 and 1/4, *Phys. Fluids*, vol. 31, pp 1007-1016, 1988.
- [13] S. Chandrasekar, *Hydrodynamics and Hydrodynamic Stability* (Oxford U. P., London), pp. 428-480, 1961.
- [14] G. I. Taylor, *Proc. R. Soc. London Ser A*, vol. 201, pp 192-oo, 1950.
- [15] Committee on High energy Density Plasma Physics Plasma Science and Committee Board of Physics and Astronomy Division on Engineering and Physical Sciences. *Frontiers in High Energy Density Physics* (The National Academies, Washington D. C., 2001)
- [16] L. F. Wang, et al, Destabilizing effect of density gradient on the Kelvin-Helmholtz instability, *Phys. Plasmas*, vol. 16, issue 11, pp 112104-112112, 2009.
- [17] N. M. Bulgakova, A. V. Bulgakov and Bobrenok, "Double layer effects in laser-ablation plasma plumes," *Phys. Rev. E*, vol. 62, issue 4, pp 5624-5635, 2000.
- [18] J. Feder and A. Aharony, *Fractals in Physics* (North Holland, Amsterdam,), 1990.
- [19] J. F. Gouyet, *Physique et Structures Fractals* (Masson, Paris, 1992).
- [20] R. Kumar, S. V. Kulkarni and D. Bora, Cylindrical stationary striations in surface wave produced plasma columns of Argon", *Phys. Plasmas*, vol 14, issue 12, pp 122101-122108, 2007.
- [21] M. Sanduloviciu and V. Melnig and C. Borcia, Spontaneously generated temporal patterns correlated with the dynamics of self-organised coherent space charge configurations formed in plasma, *Phys Letts. A*, vol. 229, issue 6, pp 354-361, 1997.
- [22] S. Gurlui, et al, Some experimental and theoretical results on the anodic patterns in plasma discharge, *Phys. Plasmas*, vol. 13, issue 6, pp 063503-063513, 2006.
- [23] S. Gurlui, et al, Experimental and theoretical investigation of a laser-produced aluminum plasma, *Phys. Rev. E*, vol. 78, issue 2, pp 026405-026414, 2008.
- [24] T. Sato, Complexity in plasma: From self-organisation to geodynamo, *Phys. Plasmas*, vol. 3, issue 5, pp 2135-2143, 1996.
- [25] R. Kumar, et al, Experimental investigation of oscillatory structures in laser-blow-off plasma plume, *Phys. Letts. A*, vol. 375, pp 2064-2070, 2011.
- [26] R. Kumar, A. Kumar, R. K. Singh, Effect of magnetic field on oscillatory structures of laser-blow-off plasma, Submitted in *Physics Letters A*.
- [27] A. Kumar, et al, Effect of ambient pressure and laser fluence on the temporal evolution of 426.7 nm CII line in laser-blow-off of multi-layered LIF-C thin film, *J. Phys. D: Appl. Phys.*, vol. 39, issue 22, pp 4860-4866, 2006.
- [28] R. K. Singh, et al, Role of ambient gas and laser fluence governing the dynamics of plasma plume produced by laser-blow-off of LIF-C thin film, *J. Appl. Phys.*, vol. 101, issue 10, pp 103301-103309, 2007.
- [29] A. Kumar, et al, An experimental setup to study the expansion dynamics of laser-blow-off plasma plume in transverse magnetic field, *Rev. Sci. Instrum.*, vol. 80, issue 3, pp 033503-033509, 2009.
- [30] A. Kumar, et al, Parametric study of expanding plasma plume formed by laser-blow-off of thin film using triple Langmuir probe, *J. Appl. Phys.*, vol 106, issue 4, pp 043306-043314, 2009.
- [31] A. Bogaerts, et al, Laser ablation for analytical sampling: what can we learn from modeling?, *Spectrochim. Acta*, Part B, vol. 58, issue 11, pp 1867-1893, 2003.
- [32] M. Murakami, et al, Ion energy spectrum of expanding laser-plasma with limited mass, *Phys. Plasma*, vol. 12, issue 6, pp 062706-062714, 2005.
- [33] P. Mora, Plasma expansion into a vacuum, *Phys. Rev. Lett.*, vol. 90, issue 18, pp 185002-185002, 2003.
- [34] K. O. Mikaelian, Normal modes and symmetries of the Rayleigh-Taylor instability in stratified fluids, *Phys. Rev. Lett.*, vol. 48, issue 19, pp 1365-1368, 1982.
- [35] K. O. Mikaelian and J. D. Lindl, Density gradients to reduce fluid instability in multishell inertial-confinement-fusion targets, *Phys. Rev. A*, vol. 29, issue 1, pp 290-296, 1984.
- [36] K. O. Mikaelian, Approximate treatment of density gradients in Rayleigh-Taylor instabilities, *Phys. Rev. A*, vol. 33, issue 2, pp 1216-1222, 1986.
- [37] O. Peromian and R. E. Kelly, Effect of density gradients in confined supersonic shear layers. I. two-dimensional disturbances, *Phys. Fluids*, vol. 8, issue 1, pp 225-240, 1996.
- [38] L. Nottale, *Fractal Space-Time and Microphysics; Towards a Theory of Space Relativity* (World Scientific, Singapore) 1993.
- [39] M. Agop and I. Rusu, El Naschie's self-organization of the patterns in a plasma discharge: Experimental and theoretical results, *Chaos, Solitons Fractals*, vol. 34, issue 2, pp 172-186, 2007.
- [40] E. A. Jackson, *Perspective of Non-linear dynamics* (Cambridge University Press, Cambridge U. K.), vols I and II, 1991.
- [41] S. J. Talasman and M. Ignat, Negative resistance and self-organization in plasmas, *Phys. Lett. A*, vol. 301, issue 1, pp 83-95, 2002.
- [42] C. Ionita, D. G. Dimitriu and R. Schrittwieser, Elementary processes at the origin ... of multiple double layers in DP machine plasma, *Int. J. Mass. Spectrum*. Vol. 233, pp 343-354, 2004.
- [43] E. Lozneau, V. Popescu and M. Sanduloviciu, Negative differential resistance related to self-organisation phenomenon in a DC gas discharge, *J. Appl. Phys.*, vol. 92, pp 1195-1200, 2002
- [44] J. Martan, O. Cibulka and N. Semmar, Nanosecond pulse laser melting investigation by IR radiometry and reflection-based methods, *Appl. Surf. Sci.*, vol. 253, issue 3, pp 1170-1177, 2006.